PROCUREMENT EXECUTIVE, MINISTRY OF DEFENCE

AERONAUTICAL RESEARCH COUNCIL

CURRENT PAPERS

Non-Linear Stability Theory of the Flat Plate Boundary Layer

by

D. Corner, M.D.J. Barry and M.A.S. Ross

Fluid Mechanics Unit, Physics Department

Edinburgh University

Communicated by Prof. D. Küchemann

Non-Linear Stability Theory of the Flat Plate Boundary Layer
- by -

D. Corner, M. D. J. Barry and M. A. S. Ross,
Fluid Mechanics Unit, Physics Department
Edinburgh University

Communicated by Prof. D. Küchemann

SUMMARY

A simultaneous solution of the non-linear stability equations for the flat plate boundary layer with space amplification has been obtained for a single non-dimensional frequency parameter, at a series of Reynolds numbers, and using a limited number of amplitudes of the fundamental perturbation. The distortion of the fundamental by the generation of second harmonic is normally included in the solution, but some results are obtained excluding this effect. The terms representing the growth of boundary layer thickness are included. The results are compared with published work on non-linear effects in plane Poiseuille flow.

1./

1. Introduction

When a steady laminar flow is perturbed by a simple harmonic disturbance
of finite amplitude the second-order processes of mean flow distortion and
generation of harmonics can be observed, at least in some types of flow, before
there are any strong indications of the random processes of turbulence. In order
to account for these second-order effects it is necessary to include in the
equations for the motion the terms that are non-linear in the perturbation and are
treated as negligible in first-order stability theory. During the last twenty
years a considerable amount of work has been done to explore the second-order
effects in various flows, both for two-dimensional and three-dimensional
perturbations. Papers by Stewartson and Stuart (1971) on the plane Poiseuille
case, and by DiPrima et al (1971) on two-dimensional flows in general, are the
latest developments of two-dimensional non-linear stability theory. These papers
give references to much of the earlier work.

Stuart (1960b) has pointed out that non-linear effects in Bénard cells
(having constant Rayleigh number), cylindrical Couette flow (having constant Taylor
number), and strictly parallel flows (having constant Reynolds number), are simpler
to analyse than non-linear effects in boundary and free shear layers which have
continuously changing Reynolds number. He has also pointed out elsewhere, however,
that if we are interested in the process of transition to turbulence there are
advantages in studying cases of changing Reynolds number, where the whole
transition process is presented as a single continuous development. It is therefore
desirable to obtain solutions of second-order perturbation equations for flows with
changing Reynolds number, and to find out by comparing theory with experiment how
far the early stages of non-linear behaviour can be followed in the transition
region. The present paper is concerned with the transition region in the Blasius
boundary layer, and develops the non-linear theory for the special experimental
case of purely real frequency and complex wave number. In this case the main
difficulty does not arise from changing Reynolds number because the undistorted
flow is of similarity type and, as will be shown below, the distortion of the mean
flow (within certain limits) does not invalidate the use of the similarity principle.
An accurate solution for this case requires the evaluation of a mean flow for which
no accurate explicit expression is possible, and also the determination of an
eigenvalue which occurs in the equation in powers up to the fourth. Numerical
methods of solution are therefore essential.

In the Blasius boundary layer the departures from parallel mean flow are
not great, and the non-linear effects are expected to be similar to those in plane
Poiseuille flow. Work on Poiseuille flow has been directed mainly to explaining
the occurrence of turbulence at Reynolds numbers R less than the critical Reynolds
number R_c given by first-order theory. The second-order changes of the rate of
amplification in both space and time have therefore been examined - for the
"subcritical" region in which $R - R_c$ is negative and for the "supercritical"
region in which $R - R_c$ is positive. Consistent results for the space amplification
case in Poiseuille flow have been given by Watson (1962) and by Stewartson and
Stuart (1971).

Interest also attaches to the second-order changes in the distribution
of the perturbation and its harmonics. Lin (1958) concluded that "for disturbances
in a parallel flow, all the harmonic components of the oscillation simultaneously
become important around the critical layer before the amplitude of the fundamental
component is large enough to cause any significant distortion of the mean flow."

The second-order results obtained for the Blasius boundary layer will be compared with those obtained for plane Poiseuille flow. Our analysis follows the method described by Barry and Ross (1970) and retains in the differential equations the main terms representing the growth of thickness of the layer. A detailed account of the numerical methods used in this work has already been published by Ross and Corner (1972).

2. The Equations and the Iteration Procedure

We use a Cartesian coordinate system having the origin in the leading edge of the flat plate, the y-axis coincident with the leading edge, and the z-axis normal to the surface of the plate. U_o represents the free-stream velocity, δ_1 the displacement thickness of the unperturbed boundary layer, and ν the kinematic viscosity of the fluid. The units of length, velocity and time are taken to be δ_1, U_o and δ_1/U_o. The equations are then non-dimensional with Reynolds number $R = U_o\delta_1/\nu$. Also $R^2 = K^2X$ where K is the Blasius constant ~ 1.7208.

The non-dimensional dependent variables include the vectors:

$(\mu, 0, \omega)$: total velocity,

$(U, 0, W)$ mean velocity,

$(u, 0, w)$ perturbation velocity,

The first equation governing the total flow in the boundary layer is the continuity equation,

$$\frac{\partial\mu}{\partial x} + \frac{\partial\omega}{\partial z} = 0,$$

which is satisfied by the introduction of a stream function ψ. The remaining equation is the vorticity equation which may be written in the form

$$\frac{\partial\ \nabla^2\psi}{\partial t} + J(\psi, \nabla^2\psi) = \frac{1}{R}\nabla^4\psi, \qquad \ldots(1)$$

where $\nabla^2\psi$ is the total vorticity, and $J(\psi, \nabla^2\psi)$ represents the operator

$$\frac{\partial\psi}{\partial z}\cdot\frac{\partial\ \nabla^2\psi}{\partial x} - \frac{\partial\psi}{\partial x}\cdot\frac{\partial\ \nabla^2\psi}{\partial z}.$$

Clearly, (1) is separable in time, and following the now well established procedure used for Poiseuille flow, the function ψ is expanded in a purely real Fourier series:

$$\psi(x,z;t) = \psi_o(x,z) + \psi_1(x,z)e^{-i\beta t} + \tilde{\psi}_1(x,z)e^{+i\beta t}$$

$$+ \sum_{n=2}^{\infty}\left[\psi_n(x,z)e^{-in\beta t} + \tilde{\psi}_n(x,z)e^{+in\beta t}\right], \qquad \ldots(2)$$

where $\sim$ indicates a complex conjugate. This expansion involves the mean flow stream function ψ_o, and $\psi_o \to \infty$ as $z \to \infty$; the expansion is valid, however,

if/

if $\psi - \psi_o$ is bounded at all times t within the range $t_o \leq t < t_o + 2\pi/\beta$. To satisfy the equations of fluid flow, ψ itself must, of course, be uniformly continuous in t, and at all real points (x,z) in the region $0 \leq z \leq \infty$, $0 < x < X$, where the positive value X can be assumed to lie outside the region of interest of this representation.

Substitution of (2) in (1), and separation in powers of $e^{i\beta t}$ gives an infinite series of equations,

$$J\left(\psi_o, \nabla^2 \psi_o\right) - \frac{1}{R} \nabla^4 \psi_o = -J\left(\tilde{\psi}_1, \nabla^2 \psi_1\right) - J\left(\psi_1, \nabla^2 \tilde{\psi}_1\right)$$

$$- \sum_{n=2}^{\infty} \left[J\left(\tilde{\psi}_n, \nabla^2 \psi_n\right) + J\left(\psi_n, \nabla^2 \tilde{\psi}_n\right) \right] \qquad \ldots (3a)$$

$$-i\beta \nabla^2 \psi_1 + J\left(\psi_o, \nabla^2 \psi_1\right) + J\left(\psi_1, \nabla^2 \psi_o\right) - \frac{1}{R} \nabla^4 \psi_1$$

$$= -J\left(\tilde{\psi}_1, \nabla^2 \psi_2\right) - J\left(\psi_2, \nabla^2 \tilde{\psi}_1\right)$$

$$- \sum_{n=2}^{\infty} \left[J\left(\tilde{\psi}_n, \nabla^2 \psi_{n+1}\right) + J\left(\psi_{n+1}, \nabla^2 \tilde{\psi}_n\right) \right] \qquad \ldots (3b)$$

$$-2i\beta \nabla^2 \psi_2 + J\left(\psi_o, \nabla^2 \psi_2\right) + J\left(\psi_2, \nabla^2 \psi_o\right) - \frac{1}{R} \nabla^4 \psi_2$$

$$= -J\left(\psi_1, \nabla^2 \psi_1\right) - J\left(\psi_3, \nabla^2 \tilde{\psi}_1\right) - J\left(\tilde{\psi}_1, \nabla^2 \psi_3\right)$$

$$- \sum_{n=2}^{\infty} \left[J\left(\tilde{\psi}_n, \nabla^2 \psi_{n+2}\right) + J\left(\psi_{n+2}, \nabla^2 \tilde{\psi}_n\right) \right] \qquad \ldots (3c)$$

$$-ni\beta \nabla^2 \psi_n + J\left(\psi_o, \nabla^2 \psi_n\right) + J\left(\psi_n, \nabla^2 \psi_o\right) - \frac{1}{R} \nabla^4 \psi_n$$

$$= - \sum_{m=1}^{n-1} J\left(\psi_m, \nabla^2 \psi_{n-m}\right)$$

$$- \sum_{m=1}^{\infty} \left[J\left(\tilde{\psi}_m, \nabla^2 \psi_{n+m}\right) + J\left(\psi_{n+m}, \nabla^2 \tilde{\psi}_m\right) \right] \qquad \ldots (3d)$$

together/

together with the complex conjugate equations of (3b), (3c) and (3d). The terms which are non-linear in the perturbation appear on the right-hand side of these equations. In first-order stability theory it is assumed that all the terms which are non-linear in the perturbation are negligible. When this assumption is made, the right-hand side in each of equations (3) becomes zero, and (3c) and (3d) become variants of (3b).

The case in which we are interested occurs when a periodic disturbance ψ_1, initially of very small amplitude, is present in the otherwise undisturbed mean flow in the boundary layer: a situation conforming initially to linearised stability theory. In consequence of boundary layer amplification, however, ψ_1 may increase in the amplifying region to such an extent that the non-linear terms in (3) become significant, distorting the mean flow given by (3a), producing higher harmonics of ψ_1 given by (3c) and (3d), and changing the function ψ_1 given by (3b). We wish to follow the early stages of this process.

It is evident from (3d) that the third and fourth harmonics cannot be excited until the second harmonic has been generated and, in general, that the (2n-1)th and 2nth cannot be excited until at least the nth has been generated. The first non-linear effects will therefore appear when the non-linear terms involving only ψ_1 just become significant in (3a) and (3c). The next stage, requiring further amplification of ψ_1, will involve terms containing ψ_1 and ψ_2 in (3b) and (3d). It will be noted that (3b) will still be linear and homogeneous in ψ_1 at this second stage. Before deciding on the number of non-linear terms which should be included in the equations for a second approximation to the solution, two simplifying assumptions must be introduced.

First, the Prandtl boundary layer assumption must be applied to the mean flow stream function ψ_0, and to do so we write

$$\nabla^2 \psi_0 = \frac{\partial^2 \psi_0}{\partial z^2} = \frac{\partial U}{\partial z} \; ; \quad \nabla^4 \psi_0 = \frac{\partial^4 \psi_0}{\partial z^4} = \frac{\partial^3 U}{\partial z^3} . \qquad \ldots (4)$$

When these substitutions are made in (3a), the left-hand side reduces to

$$\frac{\partial}{\partial z} \left[U \frac{\partial U}{\partial x} + W \frac{\partial U}{\partial z} - R^{-1} \frac{\partial^2 U}{\partial z^2} \right],$$

the partial differential with respect to z of the terms in the Blasius equation. The replacement of $\nabla^2 \psi_0$ in (3b), (3c) and (3d) retains all the terms containing W which are of the same order as the viscous term in the equation concerned. The perturbation equations then take account of the growth of boundary layer thickness (Barry & Ross, 1970).

The second assumption concerns the functions $\psi_n(x,z)$ for $n \geqslant 1$, and expresses the experimental fact that a disturbance which is periodic in time forms a wave travelling downstream within the boundary layer with a complex wave number $\alpha = \alpha_r + i\alpha_i$. $\psi_n(x,z)$ may therefore be expressed in the form $\phi_n(x,z) e^{in\alpha x}$. It is known from the work of Schubauer and Skramstad (1947) and J. A. Ross, et al (1970) that α is a function of R, and that $\phi_1(x,z)$ is a function of R and z. The dependence of ϕ_n on R may arise in two ways:

(i)   from the presence of R^{-1} as a coefficient of the viscous

   terms in the equations - and this influence is certainly

   present,

(ii) from a non-separability of x and z within ϕ_n which is

   independent of (i).

It is not possible to say a priori whether one of these is dominant or both are significant. The evidence from the work of Jordinson (1970), Barry and Ross (1970) and J. A. Ross et al indicates that, in the linearized case, (i) is dominant and that the neglect of (ii) does not lead to predictions which are erroneous within the limits of accuracy of observation. We shall therefore assume that the same conditions hold for the non-linear equations. Having found the solution of the equations based on this assumption, we may seek evidence of the existence of significant effects of (ii) in some suitable experiment. We therefore assume

$$\psi_n = C_n \phi_n(z) e^{in\alpha x}, \quad \tilde{\psi}_n = C_n \tilde{\phi}_n(z) e^{-in\tilde{\alpha}x}, \qquad \ldots(5)$$

where C_n is a real amplitude factor, and $\phi_1(z)$ is normalized so that $||\phi_1(z)|| = 1$. The position at which $\phi_1(z)$ reaches its norm is symbolized by z_n, and the normalization is carried out by making the real and imaginary parts of $\phi_1(s_n)$ respectively 1 and 0. With this normalization, $C_1 < 0.05$ will amply cover the early stages of the non-linear processes.

   The result of substituting (4) and (5) in the terms on the left-hand side of (3d) may be expressed in a concise form as

$$C_n \, e^{in\alpha x} \, G\left[\phi_n\right] \, ,$$

where

$$G\left[\phi_n\right] \equiv \left\{ \left(in\alpha U - in\beta + W\frac{d}{dz}\right)\left(\frac{d^2}{dz^2} - n^2\alpha^2\right) - \frac{1}{R}\left(\frac{d^2}{dz^2} - n^2\alpha^2\right)^2 \right.$$

$$\left. - \left(W''\frac{d}{dz} + in\alpha U''\right) \right\} \phi_n \, ,$$

and U'' and W'' are second differentials with respect to z.

Let us now suppose that for the second approximation to (3) the sum of the suffices of ϕ in any one term should not exceed 3. This rule would imply that the third harmonic is present, but with an amplitude too small to produce non-linear effects. The non-linear terms which survive on the right-hand sides of (3) will then be those involving either ψ_1 alone or ψ_1 and ψ_2. The substitution of (4) and (5) in (3) then leads to the following finite set of equations for the second approximation, where dashes represent differentiation with respect to z.

$$\frac{\partial}{\partial z}\left(U\frac{\partial U}{\partial x} + W\frac{\partial U}{\partial z} - \frac{1}{R}\frac{\partial^2 U}{\partial z^2}\right) = C_1^2 \, e^{i(\alpha - \tilde{\alpha})x}\left\{ i\alpha\left(\phi_1\tilde{\phi}_1''' - \phi_1''\tilde{\phi}_1' + (\alpha^2 - \tilde{\alpha}^2)\phi_1\tilde{\phi}_1'\right)\right.$$

$$\left. - i\tilde{\alpha}\left(\tilde{\phi}_1\phi_1''' - \tilde{\phi}_1''\phi_1' + (\tilde{\alpha}^2 - \alpha^2)\tilde{\phi}_1\phi_1'\right) \right\} \quad \ldots(6a)$$

$$C_1 \, e^{i\alpha x} \, G\left[\phi_1\right] = C_1 C_2 \, e^{i\alpha x}e^{i(\alpha - \tilde{\alpha})x}\left\{ i2\alpha\left(\phi_2\tilde{\phi}_1''' - \phi_2''\tilde{\phi}_1' + (4\alpha^2 - \tilde{\alpha}^2)\phi_2\tilde{\phi}_1'\right)\right.$$

$$\left. - i\tilde{\alpha}\left(\phi_2'''\tilde{\phi}_1 - \phi_2'\tilde{\phi}_1'' - (4\alpha^2 - \tilde{\alpha}^2)\phi_2'\tilde{\phi}_1\right) \right\} \quad \ldots(6b)$$

$$C_2 \, e^{i2\alpha x} \, G\left[\phi_2\right] = C_1^2 \, e^{i2\alpha x}\left\{ i\alpha(\phi_1\phi_1''' - \phi_1'\phi_1'') \right\} \quad \ldots(6c)$$

$$C_3 \, e^{i3\alpha x} \, G\left[\phi_3\right] = C_1 C_2 \, e^{i3\alpha x}\left\{ i2\alpha(\phi_2\phi_1''' - \phi_2''\phi_1' + 3\alpha^2\phi_2\phi_1')\right.$$

$$\left. + i\alpha(\phi_1\phi_2''' - \phi_1''\phi_2' - 3\alpha^2\phi_1\phi_2') \right\} \quad \ldots(6d)$$

In (6c) and (6d), as in the Orr-Sommerfeld equation, x disappears from the differential equation by removal of a common factor, but this will not be possible in (6a) and (6b), and a correct interpretation must be found for

exp/

$\exp i(\alpha - \tilde{\alpha})x$. In first order stability theory the downstream growth of the amplitude A for a perturbation of constant F $(= \beta/R)$ is expressed as an integral of the local rate, $-\alpha_i(R)$. Taking dimensional values $\alpha_i' = \alpha_i/\delta_1$, and $X = \delta_1^2 U_0/k^2 \nu$ (where k is the Blasius constant 1.7208), then

$$a_i' \, dX \;=\; (\alpha_i' 2\delta_1/k^2) \, d(U_0 \delta_1/\nu) \;=\; (2\alpha_i/k^2) \, dR,$$

and the total amplification between R_0 and R is

$$\frac{A}{A_0} \;=\; \exp\left[- \int_{R_0}^{R} \left(2\alpha_i/k^2\right) dR\right]. \qquad\qquad \ldots(7)$$

The appearance of the factor $\exp\left(-\alpha_i x\right)$ in a stability equation implies

that (7) is applicable. The real exponents in (6a) and (6b) represent local rates of change of the amplitude factors, C, at positions near R, but if the equations are to be integrated at R, then the C's must be given their values at R, with $x = 0$ in the exponents.

It has already been mentioned in connection with (5) that the absolute level of the values of the function ϕ_1 has been fixed by making $||\phi_1|| = 1$, and that the coefficient C_1 is the required variable amplitude factor. Equations (6c) and (6d) show that unless C_2 and C_3 are fixed in relation to C_1, the numerical values of ϕ_2 and ϕ_3 reached by integration of these equations are not fixed in relation to those of ϕ_1. (And a similar process would be reuqired for ϕ_n of higher order.) It is evident that the simplest relative normalisation for (6c) and (6d) is given by writing

$$C_n \;=\; C_1^n. \qquad\qquad \ldots(8)$$

When this relation is used with (5) in the general equation (3d) and the coefficients of the various terms are examined, we find that in all the terms on the left-hand side and the first summation on the right the co coefficient is

$C_1^n \exp\left[in\alpha_r x\right] \exp\left[-n\alpha_i x\right]$. In the second summation the typical

coefficient is $C_1^{n+2m} \exp\left[in\alpha_r x\right] \exp\left[-(n+2m)\, a_i x\right]$, where m varies

from 1 to ∞. The exponent in $i\alpha_r x$ behaves like that in $i\beta t$, and is always removable. The exponent in $-\alpha_i x$ always occurs to the same power as C_1, and merely acts as a warning that C_1 varies in the downstream direction in accordance with (7).

In order to obtain from (6) a valid second approximation to the perturbed boundary layer flow by numerical methods, it will be necessary to use four equations, (6a), (6b), (6c) and the complex conjugate of (6b); (6d) need not be involved, although its evaluation might be of interest as regards the relative magnitude of ϕ_3. (6c) shows that the second harmonic is excited by the first, and the effect of this excitation on the first harmonic should be examined.

The four equations which have to be solved are strongly coupled, and only by a process of iteration will it be possible to reach a satisfactory solution. The details of the process have been described by Ross and Corner (1972), but an outline of the method is summarised here. We begin with the first-order solutions ψ_{00} and ϕ_{10} of equations (6a) and (6b); a first-order solution of ϕ_{20} is then possible from (6c). Thereafter a second solution ψ_{01} may be obtained from (6a) using ϕ_{10} in the non-linear terms. The next stage is to recalculate ϕ_1 and its eigenvalue, including non-linear terms, and this process involves both (6b) and its complex conjugate. ψ_{01} and ϕ_{20} must be substituted to obtain ϕ_{11}. Thereafter ψ_{02} and ϕ_{21} are directly obtained from (6a) and (6c). The following diagram illustrates the route which must be followed to obtain convergent second order values of ψ_0, ϕ_1 and ϕ_2.
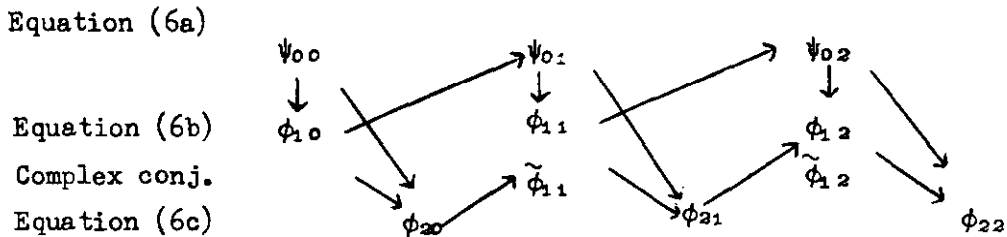
The eigenvalue solution of (6b) and its boundary conditions:

$\phi_1(0) = \phi_1'(0) = 0$, $\phi_1 \to e^{-\alpha z}$ as $z \to \infty$, was found by a special finite difference method developed by Osborne (1967) and described in its detailed operation by Ross and Corner (1972). The non-eigenvalue solutions of (6c) and (6d) and their boundary conditions: $\phi_2(0) = \phi_2'(0) = 0$, $\phi_2 \to e^{-2\alpha z}$ as $z \to \infty$, and

$\phi_3(0) = \phi_3'(0) = 0$, $\phi_3 \to e^{-3\alpha z}$ as $z \to \infty$, were found by the same finite difference method.

The solution of (6a) calls for more detailed discussion, since it is presented as a partial differential equation. The left-hand side may be reduced to a non-linear ordinary differential function of η by the method of Jones and Watson (1963), using the 'similarity' substitutions:

$$U_0 \delta_1 \psi_0 = (2\nu X U_0)^{\frac{1}{2}} f(\eta); \qquad \eta = (U_0/2\nu X)^{\frac{1}{2}} z,$$

with $X = x \delta_1$, $Z = z \delta_1$, and $\delta_1 = k (\nu X/U_0)^{\frac{1}{2}}$, the constant k having the Blasius value 1.7208 (to five significant figures). Then introducing the homologous substitution:

$$f(\eta) = 2^{\frac{1}{2}} k^{-1} F(2^{\frac{1}{2}} k^{-1} \eta) = 2^{\frac{1}{2}} k^{-1} F(z),$$

(6a) reduces to

$$F^{iv}(z) + F'''(z) F(z) + F''(z) F'(z) = -\tfrac{1}{2} k^2 R C_1^2 D(z)$$

$$= \mathcal{D}(z), \qqu\qquad ...(9)$$

where $C_1^2 D(z)$ represents the right-hand side of (6a) with the exponent absorbed into C_1^2.

The use of the similarity principle implies an x-dependence as well as a z-dependence in the whole equation, but since the integration is performed at constant x, and is valid only at one value of x, the implied x-dependence in the right-hand side may be ignored.* The solutions of (9) were found by the Runge-Kutta method, using the boundary conditions $F(0) = F'(0) = 0$, $F'(\infty) = 1$, $F''(\infty) = 0$.

It is necessary to enquire, however, under what conditions there will exist a valid solution of (9). If C_1 is sufficiently small, a valid solution will exist, differing inappreciably from the Blasius profile. The addition of the distortion term is not unacceptable unless it leads to an unacceptable distribution $U = f'(\eta)$. The limitations involved appear to be similar to those which apply to the Pohlhausen parameter, which is subject to upper and lower limits. In the present case we assume that there is an upper limit to C_1 for given R and F. The first indications that a limit of this kind existed was found in the solution of (6a) for $R = 500$, $F = \beta/R = 0.00008$, $C_1 = 0.056$. The calculated values of U were then found to exceed unity by at most 27 parts in 10^9 around $z = 4.5$. The numerical solutions were found for the range $0 \leqslant z \leqslant 6$ divided by the net points into 80 equal intervals, and the boundary conditions were applied at the two ends of the range. Tests were performed to ensure that the net was sufficiently fine and that the outer limit of z was sufficiently large. The calculations were performed on the I.C.L.4/70 Computer at the Edinburgh Regional Computer Centre. The time required by the program was about 10 seconds per cycle of (6a), (6b) and (6c). Recycling was terminated when results became stable in the seventh significant figure.

All the calculations were performed for $F = \beta/R = 0.00008$, and for various values of R and C_1. The components of the cycle had second order convergence, but the recycling iteration was first order. Application of an Aitken δ^2-correction to both the eigenvalue and eigenvector was found to assist convergence. Table 1 shows the number of cycles of iteration required under various conditions.

Table 1

Number of Cycles of Iteration Required for
Various Values of R and C_1 at $F = 80 \times 10^{-8}$

R \ C_1	0.007	0.014	0.028	0.056
500	-	-	6	15
800	-	-	9	-
1000	-	6	12	-
1250	-	9	-	-
1500	-	16	-	-
1750	12	-	-	-

3./

* The x-dependence in the mean flow is very small and is usually neglected in boundary layer stability theory. It enters here because the growth of boundary thickness has been included. A treatment similar to ours was used by Pretsch (1941) in his paper on boundary layers with a pressure gradient.

3. Results of the Calculations

In order to give a general view of the results, selected data are presented in three tables representing respectively the first damping region $(R = 500)$, the amplifying region $(R = 1000)$, and the second damping region $(R = 1750)$. The data given in these tables are all dimensionless, and the unit of length involved is the Blasius value of δ_1 corresponding to the Reynolds number concerned. The presence of the perturbation affects the displacement thickness, and the changed value is represented non-dimensionally by δ_1^*. To present the complex fluctuating functions in a physically meaningful way they have been reduced to the form of modulus and argument for $\alpha_r x - \beta t = 0$. The tables show only the moduli of normalised functions. To obtain the corresponding non-dimensional r.m.s. values, the tabulated data for the first, second and third harmonics of the perturbation should be multiplied respectively by $2^{\frac{1}{2}}C_1$, $2^{\frac{1}{2}}C_1^2$ and $2^{\frac{1}{2}}C_1^3$.

Table 2

Computed Values with $R = 500$, $F = 80 \times 10^{-6}$

C_1	0	0.028	0.056	
δ_1^*	1.000	0.987	0.945	non-dimensional
z $(U=0.99)$	2.854	2.801	2.613	
α_r	0.12298	0.12299	0.12309	
α_i	+0.016734	+0.017069	+0.017970	
c_r	0.3194	0.3191	0.3182	
z_c	0.5625	0.5568	0.5378	
z_m	0.8674	0.8676	0.8679	z for $|\phi_1'|_{max}$
z_n	2.443	2.414	2.313	phase reversal of ϕ_1'
$|\phi_1'|_{max}$	0.7498	0.7552	0.7740	
$|\phi_2'|_{max}$	2.2740	2.2206	2.1011	
$|\phi_3'|_{max}$	9.187	8.656	7.445	
$|\nabla^2\phi_1|_{max}$	0.6998	0.7206	0.7943	near 2.5 z_c
$|\nabla^2\phi_2|_{max}$	4.044	3.996	3.899	near 1.5 z_c
$|\nabla^2\phi_3|_{max}$	20.48	19.63	17.74	near z_c

The data in Table 2 show the following characteristics of the first damping region.

(i) As C_1 is increased, changes in α_i, the local rate of damping, are small, and the amount of energy transferred to the mean flow must increase. In consequence, the thickness of the boundary layer decreases as shown by both δ_1^*, the non-dimensional displacement thickness, and the value of z for $U = 0.99$.

(ii)/

(ii) The value of α_r increases slightly with increasing C_1, and since the frequency is constant, the wavelength and the wave velocity, c_r, decrease.

(iii) As a result of both (i) and (ii), the value of z at the critical point, z_c, decreases quite significantly. Associated with the inward movement of z_c there is a similar inward movement of z_n, the position of phase reversal in the downstream component of the perturbation velocity.

(iv) Since ϕ_1 is normalised in such a way that $\int_0^{z_n} |\phi_1'| \, dz \approx 1$, the inward movement of z_n causes the peak value of $|\phi_1'|$ to rise. It is interesting to note, however, that as C_1 increases the peak values of $|\phi_2'|$ and $|\phi_3'|$ decrease. The relatively high ratio of $|\phi_2'|_{max}$ and $|\phi_3'|_{max}$ to $|\phi_1'|_{max}$ accounts for the development of a cascade of harmonics as C_1 increases.

(v) For all the harmonics the modulus of vorticity has its highest value at the flat plate. As z increases this modulus falls steeply to a minimum and then rises to a secondary maximum. The table shows the peak value of the secondary maxima with a rough indication of the z-position expressed in terms of z. The data show the rapid growth of the normalised functions with increasing order of harmonic and a slight tendency to suppression of higher harmonics as C_1 increases.

Table 3

Computed Values with $R = 1000$, $F = 80 \times 10^6$

C_1	0	0.014	0.028	
δ_1^*	1.000	1.004	1.014	non-dimensional
z (U=0.99)	2.854	2.860	2.872	
α_r	0.23046	0.22883	0.22461	
α_i	-0.006605	-0.006083	-0.005162	
c_r	0.3468	0.3494	0.3560	
z_c	0.6120	0.6189	0.6371	
z_m	0.6241	0.6389	0.6770	z for $|\phi_1'|_{max}$
z_n	2.108	2.123	2.172	phase reversal of ϕ_1'
$|\phi_1'|_{max}$	0.7929	0.7819	0.7543	
$|\phi_2'|_{max}$	8.052	7.511	6.196	
$|\phi_3'|_{max}$	77.48	66.94	44.87	
$|\nabla^2\phi_1|_{max}$	0.7150	0.7104	0.7007	near $2\,z_c$
$|\nabla^2\phi_2|_{max}$	12.61	11.71	9.56	near z_c
$|\nabla^2\phi_3|_{max}$	157.4	137.0	95.0	near z_c

The data in Table 3 show the following characteristics of the amplifying region.

(i) As C_1 is increased, α_i remains negative (although diminishingly so), and the resulting amplification of the perturbation involves the removal of energy from the mean flow. The thickness of the boundary layer is progressively increased, as shown by both δ_1^* and the value of z for $U = 0.99$. The fractional increase in δ_1^* for $C_1 = 0.028$ is comparable with the fractional decrease at $R = 500$ for the same amplitude, but the total thickness of the layer appears less sensitive to expanding than to contracting influences.

(ii) The value of α_r decreases slightly with increasing C_1, and the wavelength and c_r increase. For $C_1 = 0.028$ the proportional increase in c_r is much larger than the proportional decrease at $R = 500$.

(iii) As a result of both (i) and (ii), the value of z_c increases with increasing C_1. The fractional increase is bigger at $R = 1000$ than the corresponding decrease at $R = 500$ for the same amplitude. Associated with the outwards movement of z_c there are similar movements of z_n and (more definitely) z_m.

(iv) The outwards movement of z_n causes the peak value of $|\phi_1'|$ to fall slightly. The peak values of $|\phi_2'|$ and $|\phi_3'|$ are more markedly reduced as C_1 increases. At small amplitudes there is a large increase in the ratio of $|\phi_2'|_{max}$ and $|\phi_3'|_{max}$ to $|\phi_1'|_{max}$ by comparison with the data for $R = 500$.

(v) The secondary peaks in the vorticity distributions show a similar intensification in the higher harmonics at low amplitude, and similar diminution with increasing C_1. These vorticity peaks lie somewhat closer to z_c than do those at $R = 500$.

Table 4

Computed Values with $R = 1750$, $F = 80 \times 10^{-6}$

C_1	0	0.007	
δ_1^*	1.0000	0.9983	non-dimensional
z $(U=0.99)$	2.856	2.846	
α_r	0.38444	0.38355	
α_i	+0.02631	+0.01718	
c_r	0.3625	0.3643	
z_c	0.6403	0.6450	
z_m	0.2485	0.2458	z for $|\phi_1'|_{max}$
z_n	1.736	1.735	phase reversal of ϕ_1'
$|\phi_1'|_{max}$	1.0421	1.0345	
$|\phi_2'|_{max}$	5.619	4.154	
$|\phi_3'|_{max}$	105.6	54.02 and 59.47	
$|\nabla^2\phi_1|_{max}$	1.691	1.378	near $1.2\, z_c$
$|\nabla^2\phi_2|_{max}$	42.6	26.3	near $1.1\, z_c$
$|\nabla^2\phi_3|_{max}$	1204	671.7	near $1.2\, z_c$

The/

The data in Table 4 show the following characteristics of the second damping region in the initial stage of increasing C_1.

(i)   The thickness of the boundary layer decreases, as in the first damping region.

(ii) c_r increases as in the amplifying region.

(iii) z_c moves outwards as in the amplifying region.

(iv)   Although z_n seems almost constant, $|\phi_1'|_{max}$ decreases as in the amplifying region. Very large decreases occur with increasing C_1 in $|\phi_2'|_{max}$ and $|\phi_3'|_{max}$, but the small amplitude values have ratios similar to those at $R = 1000$.

(v)   The secondary peaks in the vorticity distributions show much larger harmonic development at low amplitude than those at $R = 1000$. Considering the small size of the finite amplitude used in Table 4, the decrease in the harmonic peaks is striking. All the peaks are now found close to z_c.

Having shown in Tables 2, 3 and 4 the effects of changing C_1 in the three main regions of the field it will now be useful to show the distributions through the boundary layer of various functions derived from the solutions of (6) for $F = 0.00008$ in each region. Because of the rapidly varying stability of the numerical analysis with increasing R and C_1, different values of C_1 are selected for illustration at different values of R. Graphs are shown in Fig.1 for $R = 500$, $C_1 = 0.028$, in Fig.2 for $R = 1000$, $C_1 = 0.014$, and in Fig.3 for $R = 1750$, $C_1 = 0.007$. Each figure contains eight graphs showing the following functions of z:

(a)   The normalised functions $|\phi_1|$ and $|\phi_1'|$.

(b)   The normalised functions $|\phi_2|$ and $|\phi_2'|$.

(c)   The normalised functions $|\phi_3|$ and $|\phi_3'|$.

(d)   The fractional local distortion of the mean flow, $(U - U_B)/U_B$,

and $(W - W_B)/W_B$, where U and W represent the distorted flow

and U_B and W_B are the corresponding Blasius values.

(e)   The r.m.s. values of the four largest terms in (6b). For this graph we
write $h_1 = 2^{\frac{1}{2}}C_1 |\nabla^2\phi_1|$. The four rate-of-change of vorticity terms
are then βh_1, $U|\alpha|h_1$, $- U''|w_1|$, and $R^{-1}h_1''$, where w_1 represents the
normal velocity component of the fundamental perturbation, and
$h_1'' = 2^{\frac{1}{2}}C_1 |d^2(\nabla^2\phi_1)/dz^2|$.

(f)   The arguments of the first three terms noted in (e).

(g)   The r.m.s. second harmonic vorticity modulus, $h_2 = 2^{\frac{1}{2}}C_1^2 |\nabla^2\phi_2|$.

(h)   The r.m.s. third harmonic vorticity modulus, $h_3 = 2^{\frac{1}{2}}C_1^3 |\nabla^2\phi_3|$.

To convert from normalised to r.m.s. values, the ordinates should be multiplied in
(a) by $2^{\frac{1}{2}}C_1$, in (b) by $2^{\frac{1}{2}}C_1^2$, and in (c) by $2^{\frac{1}{2}}C_1^3$.

In two-dimensional stability theory the perturbation vorticity behaves like a scalar quantity and is the simplest property which can be used to visualise the disturbance process. The graphs (e) and (f), showing the only terms of any importance in (6b), reveal this simplicity. Since the arguments represent the phase angles when $a_r x - \beta t = 0$, the phase angles at any (x,z) position rotate in the clockwise direction with increasing t.

The dotted curves in the (f) graphs show that the phase angle of w_1 near the plate has a progressively increasing lag as z increases, corresponding to the diffusion of perturbation vorticity from the source at the plate surface, and the expected, almost constant phase in the outer part of the layer. It is known from other results (not shown in the Figures) that the fundamental u component lags about $90°$ behind the w component until the phase reversal point z_n is approached. The phase reversal in the damping region takes place in the clockwise direction, and in the amplifying region normally in the counterclockwise direction.

The continuous curves in the (f) graphs, representing $\arg(\beta \nabla^2 \phi_1)$, show a phase reversal of the fundamental vorticity in the region of the critical point, z_c. In the outer part of the layer our results predict an almost constant phase angle. In all cases the wave front is very slightly tilted forwards towards the outer edge of the layer. Table 6 shows approximate values of this forward tilt in degrees per unit distance δ_1.

Table 5

Approximate Slope of the Wave Front at the Outer Edge of the Boundary Layer in Degrees per Distance δ_1

R \ c_1	0	0.007	0.014	0.028	0.040	0.056
500	17.8	-	-	20.9	-	32.6
800	-	-	-	8.5	9.8	-
1000	4.6	-	4.7	5.2	-	-
1250	-	-	2.9	-	-	-
1500	-	-	2.3	-	-	-
1750	3.3	2.7	-	-	-	-

4. Comparison with Other Theoretical Work

In a discussion of the "multiplicity" of the non-linear effects examined in earlier work, Lin (1958) applied an order of magnitude argument to establish the special importance of the critical layer for the transport of vorticity. He used a length parameter derived from the ratio of the convection to the viscous terms in the dimensional Orr-Sommerfeld equation, and concluded that "the non-linear effect first shows up in the generation of harmonic modes in the critical layer even before the distortion of the mean flow is noticeable." Here we wish to comment on this conclusion from a theoretical standpoint.

It will be seen that our Equations (6a) and (6b) necessarily involve the amplitude factor C_1^2 in their non-linear terms, and the calculated distorted mean flow and fundamental perturbation are directly dependent on C_1^2. In Equations (6c) and (6d), on the other hand, the amplitude factors C_1^2 and C_1^3 cancel out, and normalised solutions are obtained which depend on C_1 only through ψ_0 and ϕ_1. Thus ϕ_2 and ϕ_3 may be calculated even if $C_1 = 0$, and the higher harmonics must therefore be regarded as inherent features of the perturbation. This argument is not weakened by the evidence in Tables 2 to 4 that the peak values of the normalised functions derived from ϕ_2 and ϕ_3 decrease as C_1 increases. As R increases, however, the distribution of the r.m.s. vorticities h_2 and h_3 becomes progressively more concentrated near $z = 0$ and $z = z_c$ (c.f. Figs. 1(g), 2(g), 3(g) and 1(h), 2(h), 3(h)). The peak values of the corresponding normalised functions rise steeply as R increases (Tables 2 to 4).

Lin's argument was concerned with the case when the dimensional equivalent of $(\alpha R)^{1/3}$ was large, and we regard our results as consistent with his conclusions - interpreted in the sense that the harmonics contribute in an essential way to the perturbation processes in the viscous region. In discussing this question we are not concerned with the e experimental detectability of the different non-linear effects; this naturally depends on the value of C_1, but depends also on the relative ease of observation of a.c. and d.c. signals.

It may also be of interest to compare our results in a general way with those obtained in non-linear studies of plane Poiseuille flow. In a series of papers initiated by Meksyn and Stuart (1951), and including notably Stuart (1960a), Watson (1960, 1962), Reynolds and Potter (1967), Pekeris and Shkoller (1967) and Stewartson and Stuart (1971), a theory has been developed to express the effect of the non-linear terms on the rate of amplification and damping of perturbations, and the formal expressions have been evaluated numerically. The theory was originally developed for amplification in time, but Watson (1962) and Stewartson and Stuart have given the corresponding relation for space amplification.

It will be sufficient here to consider the real part of the amplification Equation (5.1) of Stewartson and Stuart for our real amplitude and fixed frequency parameter:

$$\frac{1}{2}\frac{\partial}{\partial x}\left(\ln|A|^2\right) = -\alpha_i(C_1,R) = -\alpha_i(0,R) + \frac{k_r}{c_g}|A|^2, \qquad \ldots(10)$$

where $|A|^2 = 4C_1^2$, c_g is the local group velocity, and k_r is a local constant expressing in magnitude and sign the contribution to α_i from the non-linear terms. In the amplifiing region $\alpha_i(0,R)$ is negative, and the instability is increased when k_r is positive and decreased when k_r is negative. In the damping regions $\alpha_i(0,R)$ is positive, and the stability is increased when k_r is negative and decreased when k_r is positive. Thus when $\alpha_i(0,R)$ and k_r have the same sign of $\alpha_i(C_1,R)$ may become

opposite to that of $\alpha_i(0,R)$ if $|A|^2$ is sufficiently large. Table 6 shows the values of k_r/c_g obtained from our values of α_i, and the values of c_g derived from calculations of $\partial\alpha/\partial\beta$ at constant R.

Table 6

Second Order Changes in α_i at $F = \beta/R = 80 \times 10^6$

R	$A = \dfrac{2C_1}{c}$ %	$\alpha_i \times 10^4$	k_r/c_g	$(k_1 + k_3)/c_g$	k_2/c_g	c_g
500	0	+167.34	-	-	-	0.4022
	2.8	+168.20	- 0.1102	-	-	
	5.6	+170.69	- 0.1067	+ 0.0255	-0.1322	
	11.2	+179.73	- 0.0988	-	-	
800	0	+ 6.92	-	-	-	0.4155
	2.8	+ 10.99	- 0.5198	-	-	
	5.6	+ 20.57	- 0.4351	+ 0.0693	-0.5044	
	8.4	+ 30.23	- 0.3303	-	-	
1000	0	- 66.05	-	-	-	0.4112
	1.4	- 64.59	- 0.7444	-	-	
	2.8	- 60.83	- 0.6651	- 0.2043	-0.4608	
	5.6	- 51.62	- 0.4600	-	-	
1250	0	- 80.58	-	-	-	0.4058
	1.4	- 81.08	+ 0.2576	-	-	
	2.8	- 81.71	+ 0.1433	- .3666	+0.5099	
	4.2	- 81.23	+ 0.0367	-	-	
	5.6	- 79.31	- 0.0406	-	-	
1500	0	+ 22.22	-	-	-	0.4028
	1.4	+ 6.62	+ 7.956	+ 5.930	+2.026	
	2.8	- 18.97	+ 5.255	-	-	
	4.2	- 36.30	+ 3.318	-	-	
1750	0	+263.15	-	-	-	0.4371
	0.7	+232.04	+63.49	+64.67	-1.182	
	1.4	+171.79	+46.61	-	-	
	2.8	+ 77.35	+23.70	-	-	

At an early stage in the present work, simultaneous solutions were obtained for (6a) and (6b) with ϕ_2 treated as negligible. This procedure gives the distorted mean flow and the consequent modification of ϕ_1 and its eigenvalue, and thus gives the combined effect of the parameters k_1 and k_3 (Stuart, 1960a). Column 5 in Table 6 is found by inserting the resulting values of α_i in (10). Column 6 is found by subtracting column 5 from column 4. (It should be noted that all the values of k/c_g correspond in their scale to $a^{(2)}$ as used by Reynolds and Potter and McIntire and Lin, and $k_1 + k_3$ and k_2 are not given at double the $a^{(2)}$ scale.).

Because of the departures from constancy of k_r when two values of C_1 were used at a given R, the accuracy of α_i was tested at R = 800. The calculations were performed with 80, 120 and 160 net points in the range $0 \leqslant z \leqslant 6$, and extrapolated to an infinite number of net points using the fourth power of interval size. The values of k_r/c_g then became less negative, but only by about 2.3%. The variations of k_r/c_g are therefore considered to be reliable.

For our value of F, branches I and II of the neutral stability curve lie near R = 815 and R = 1465. The values of α_i in Table 6 show that when R is 500, 800 and 1000, and the linearised equations give increasing instability as R increases, the non-linear effects make the boundary layer more stable or less unstable. When R is 1500 and 1750, and the linearised equations give increasing stability as R increases, the non-linear effects act in the opposite direction and make the boundary layer less stable. The non-linear effects thus tend to maintain a more constant periodic oscillation. At R = 1250 the amplitude-dependent changes are almost negligible. Qualitatively similar results have been obtained for time-amplified disturbances in plane Poiseuille flow by Pekeris and Shkoller (1967, 1969) and by McIntire and Lin (1972) in their Table 1.

If we examine the relative values of k_r, $k_1 + k_3$ and k_2, we find that k_2 is the dominant influence in k_r at the three lowest Reynolds numbers and that $k_1 + k_3$ is dominant at the two highest Reynolds numbers. It therefore appears that the amplitude-dependent increase of damping at low Reynolds numbers occurs mainly because of gain of energy by the harmonics. Equations (3) show that the higher harmonics are generated by those of lower order. The omission of the higher harmonics from our calculations is therefore likely to lead to an underestimate of the changes in α_i at low Reynolds numbers.

At the two highest Reynolds numbers the situation is different; the predominant contribution to k_r comes from $k_1 + k_3$ which represents the mean flow distortion. When α_i is positive in this region and the fundamental is losing energy, the energy is mainly transferred in the first instance to the mean flow, and thus only indirectly to the higher harmonics which are known to develop in this region. Thus, although as shown in Fig.3(d) the percentage changes in U and W are small, these changes must be significant for the breakdown of laminar flow. It has been found be Pekeris and Shkoller for plane Poiseuille flow that high eigenstates which are subject to damping in time, and are a function of the mean flow, contribute to changes

resembling/

resembling breakdown. This suggests that a careful study should be made of the higher eigenstates in the space-amplification conditions of the Blasius boundary layer. Some preliminary work has shown that such states exist in the Blasius layer, and that the Reynolds numbers at which they first appear is sensitive to the inclusion in the equations of the terms representing the normal velocity component of the mean flow.

5. Possible Extensions of the Calculations

In addition to finding solutions of (6) for particular sets of values of R, F and C_1, it is possible to find curves corresponding to those found in linearised theory, namely,

(i) the neutral stability curve, and

(ii) the growth of amplitude of a perturbation in the downstream direction.

Curves of both kinds have been found by Pekeris and Shkoller (1969) for the non-linear stability of plane Poiseuille flow with time amplification.

From the point of view of comparison with experiment in boundary layers, curve (ii) is of particular interest. In the small amplitude case where α_i is not a function of C_1, the curve is obtained by determining α_i at a series of values of R which are sufficiently closely spaced to permit accurate integration of the area under the curve of α_i versus R using (7). When larger amplitude coefficients are used and α_i becomes a function of C_1, the integration must take account of the simultaneously changing values of C_1 and R, and the intervals ΔR must be chosen to limit the errors in the numerical integration. If $C_1^{(j)}$ is the amplitude coefficient at R_j, then the simultaneous solution of (6) gives $\alpha_i^{(j)}$. We then find

$$C_1^{(j+1)} = C_1^{(j)} \exp\left(2\Delta R_j \alpha_i^{(j)}/k^2\right)$$ and solve (6) for the next interval with

the new value of C_1 and R_{j+1}. The error in this integration is controlled in terms of the second order differences of α_i as a function of R.

The procedure which must be followed in the case of space amplification of a wave of fixed frequency travelling through a region of changing R is quite different from that used in the case of time amplification of a wave of fixed real wave number at constant R. The Orr-Sommerfeld equation, and the system of equations representing non-linear stability have a very simple time dependence, but a very complicated x and R dependence.

Acknowledgements

References/

References

Barry, M. D. J. and Ross, M. A. S.	1970	J. Fluid Mech. 43, 813.
Di Prima, R. C., Eckhaus, W. and Segel, L. A.	1971	J. Fluid Mech. 49, 705.
Jones, C. W. and Watson, E. J.	1963	In Laminar Boundary Layers. Oxford University Press.
Lin, C. C.	1958	Boundary Layer Research, p.144. I.U.T.A.M. Symposium, Freiburg, 1957 (editor, H. Gortler). Berlin: Springer.
McIntire, L. V. and Lin, C. H.	1972	J. Fluid Mech. 52, 273.
Meksyn, D. Stuart, J. T.	1951	Proc. Roy. Soc. A 208, 517.
Osborne, M. R.	1967	SIAM J. Appl. Math. 15, 539.
Pekeris, C. L. and Shkoller, B.	1967	J. Fluid Mech. 29, 31.
Pekeris, C. L. and Shkoller, B.	1969	J. Fluid Mech. 39, 629.
Pretsch, J.	1941	Jb. dtsch. Luftfahrtf. 1, 158.
Reynolds, W. C. and Potter, M. C.	1967	J. Fluid Mech. 27, 465.
Ross, M. A. S. and Corner, D.	1972	Proc. Roy. Soc. Edinb. A.70, 251.
Schubauer, G. B. and Skramstad, H. K.	1947	J. Res. Nat. Bur. Stand, 38, 251.
Stewartson, K. and Stuart, J. T.	1971	J. Fluid Mech. 48, 529.
Stuart, J. T.	1960a	J. Fluid Mech. 9, 353.
Stuart, J. T.	1960b	Non-linear effects in hydrodynamic stability. Proc. Xth Internat. Congress of Appl. Mech. Stresa.
Watson, J.	1960	J. Fluid Mech. 9, 371.
Watson, J.	1962	J. Fluid Mech. 14, 221.

Legends for Figures

Fig.1 Distributions for $R = 500$, $C_1 = 0.028$, $F = 80 \times 10^{-6}$.
(a) Normalised $|\phi_1(z)|$ and $|\phi_1'(z)|$; (b) normalised $|\phi_2(z)|$
and $|\phi_2'(z)|$; (c) normalised $|\phi_3(z)|$ and $|\phi_3'(z)|$; (d) fractional
change of the mean flow (per cent), ——— downstream component,
------ normal component, (U_B, W_B) the Blasius flow.

Fig.1 Distributions for $R = 500$, $C_1 = 0.028$, $F = 80 \times 10^{-6}$.
(e) r.m.s. values (per cent) of the four largest terms in equation
(6b), ——— βh_1, ------ $U|\alpha|h_1$, ... $-U''|w_1|$,
x x x x x $R^{-1}h_1''$, h_1 = r.m.s. vorticity of the fundamental;
(f) arguments of the first three curves in (e); (g) h_2 = r.m.s.
vorticity of the second harmonic; (h) h_3 = r.m.s. vorticity of the
third harmonic.

Fig.2 Distributions for $R = 1000$, $C_1 = 0.014$, $F = 80 \times 10^{-6}$.
(a), (b), (c), (d) as in Fig.1.

Fig.2 Distributions for $R = 1000$, $C_1 = 0.014$, $F = 80 \times 10^{-1}$.
(e), (f), (g), (h) as in Fig.1.

Fig.3 Distributions for $R = 1750$, $C_1 = 0.007$, $F = 80 \times 10^{-6}$.
(a), (b), (c), (d) as in Fig.1.

Fig.3 Distributions for $R = 1750$, $C_1 = 0.007$, $F = 80 \times 10^{-6}$.
(e), (f), (g), (h) as in Fig.1.

BW
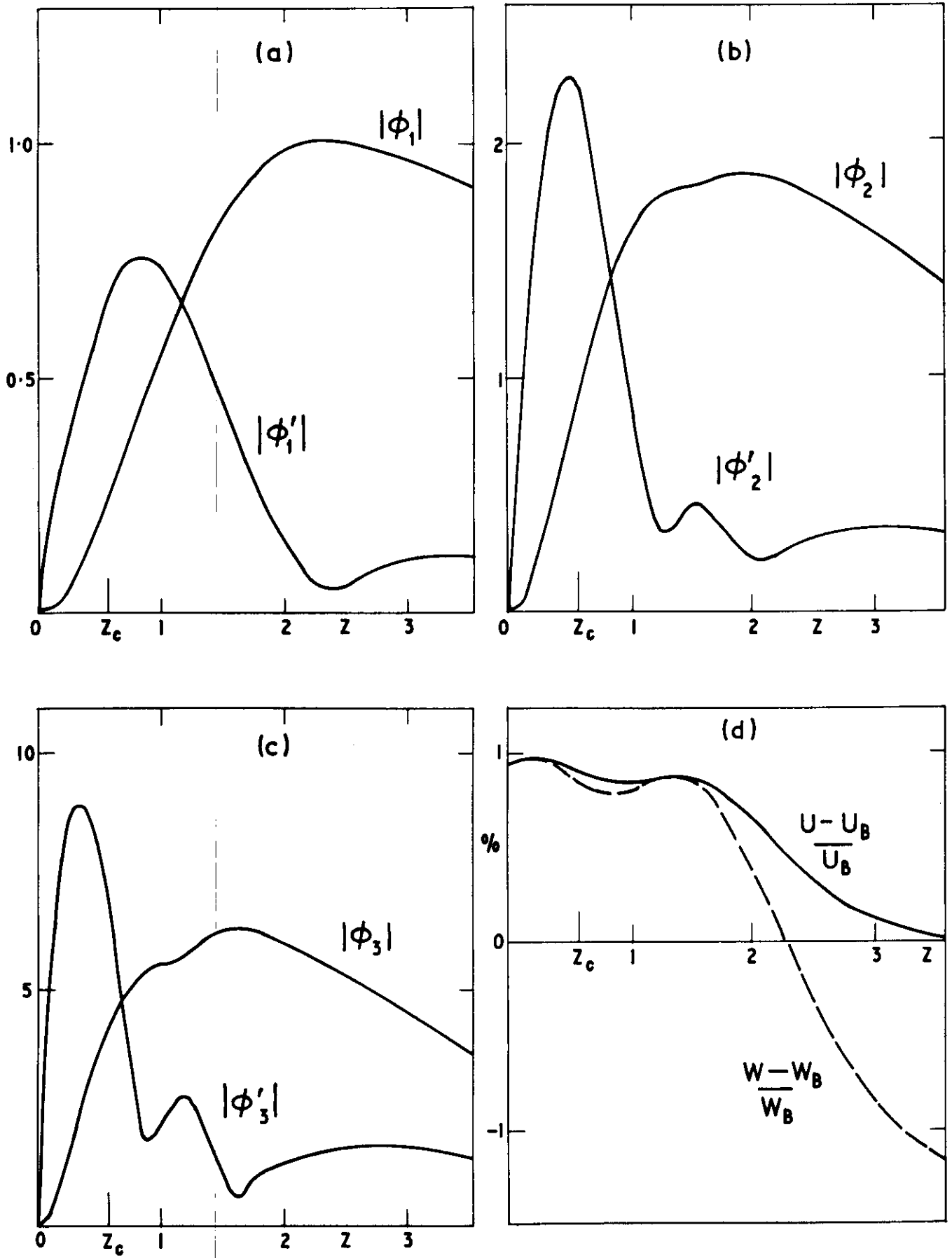
FIG. 1.
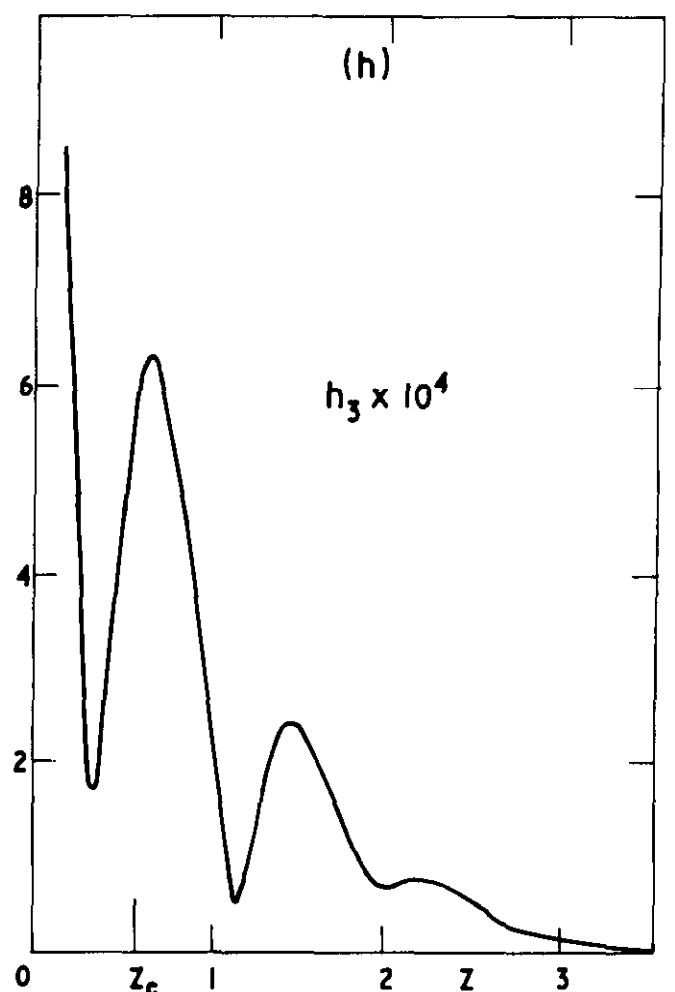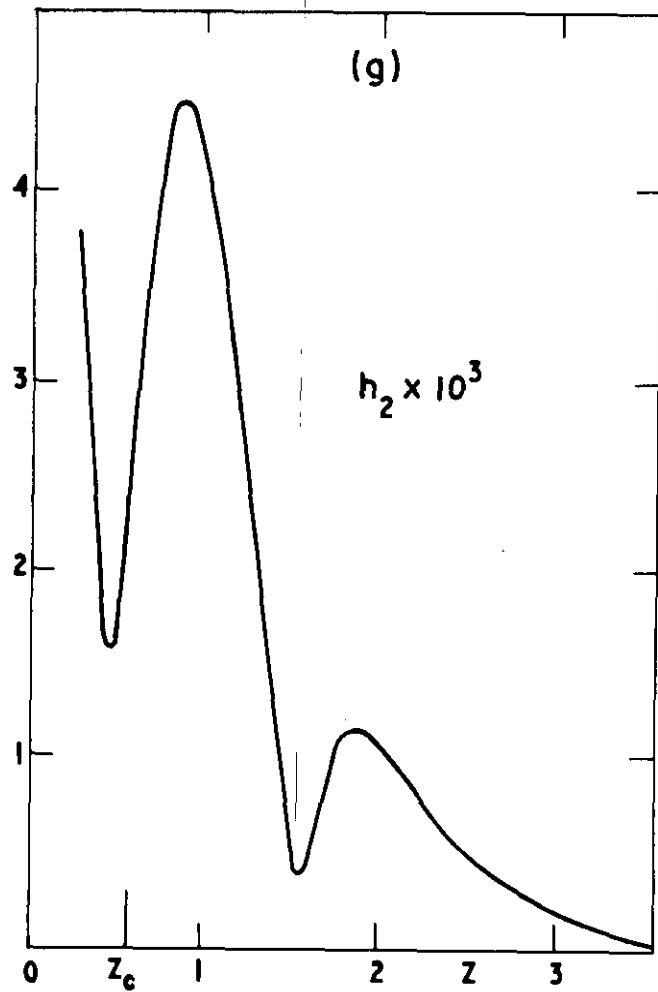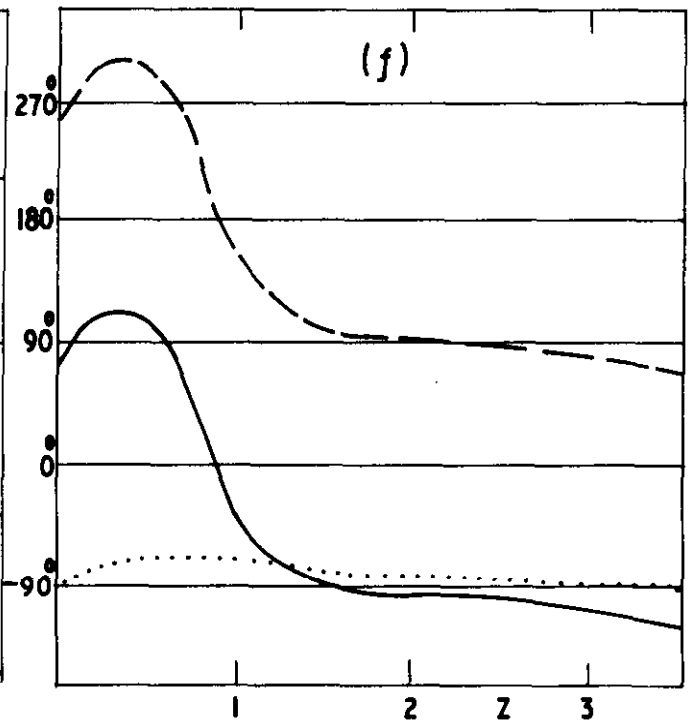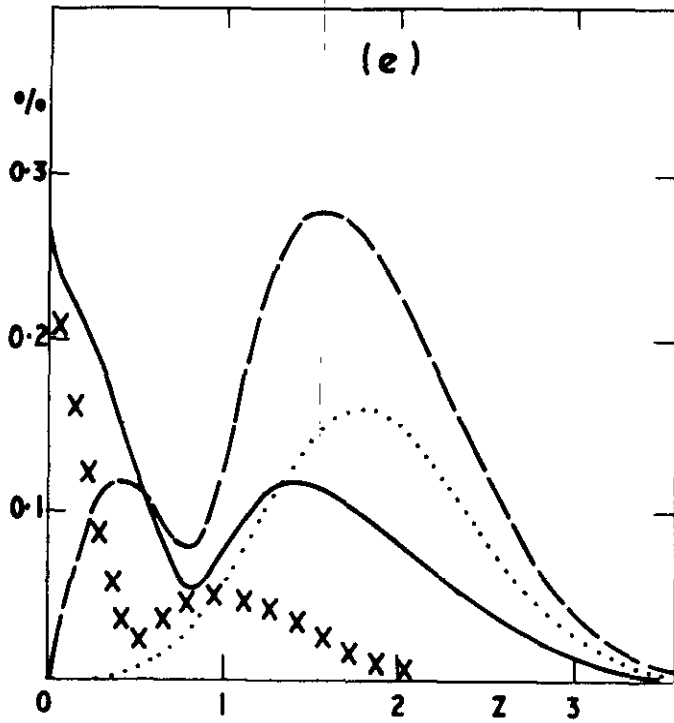
FIG.1 (cont.)
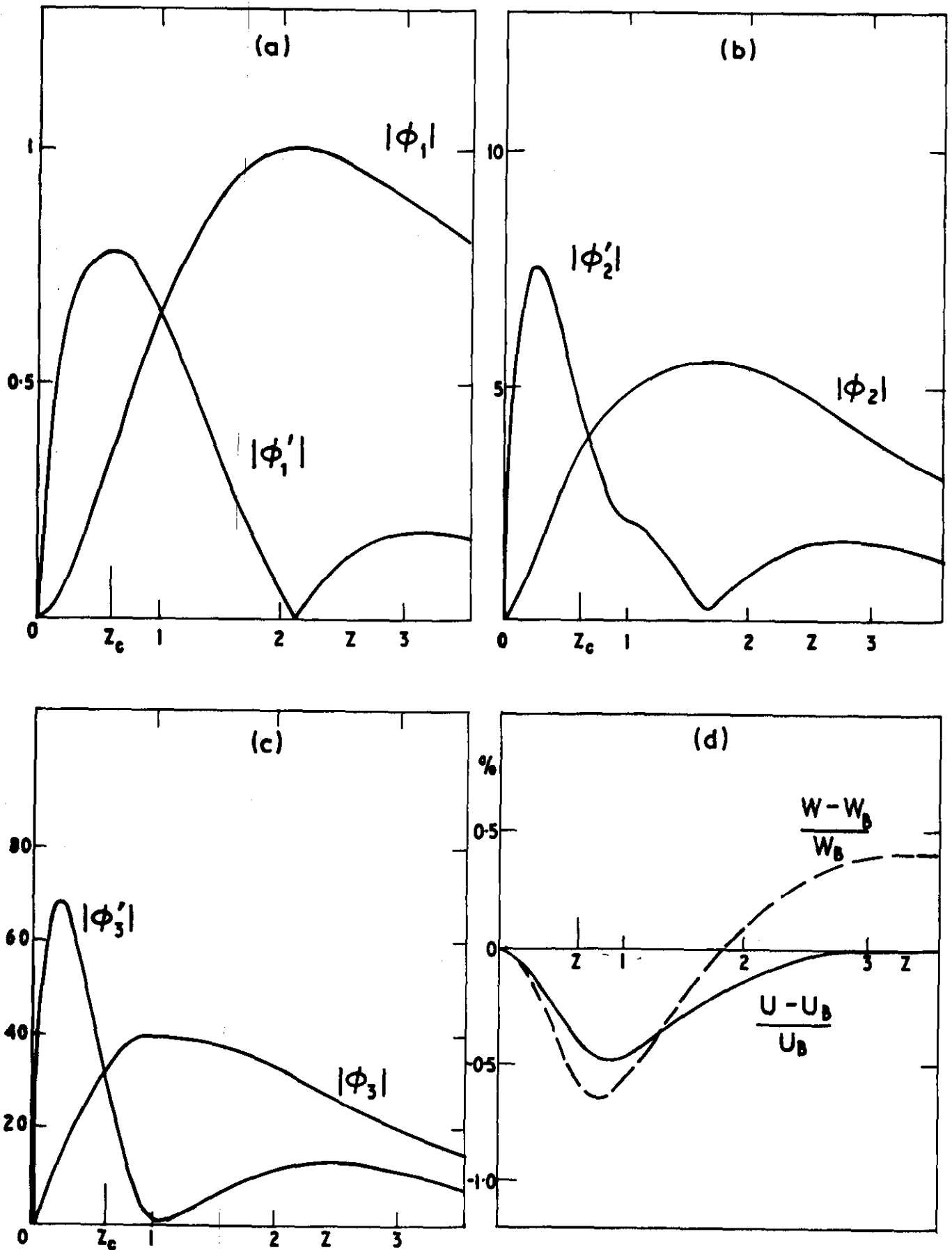
FIG.2
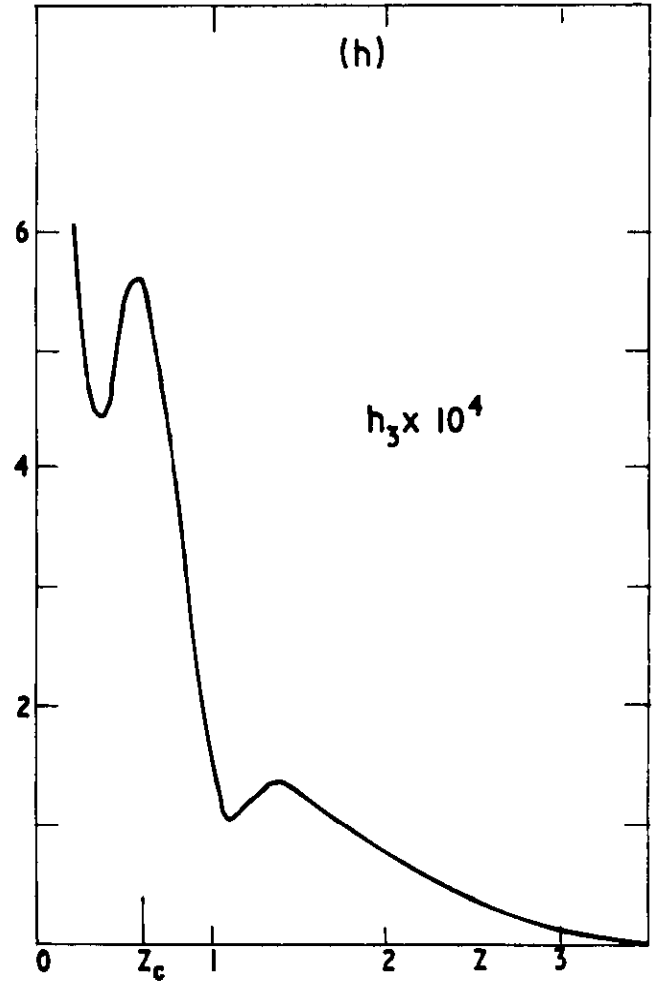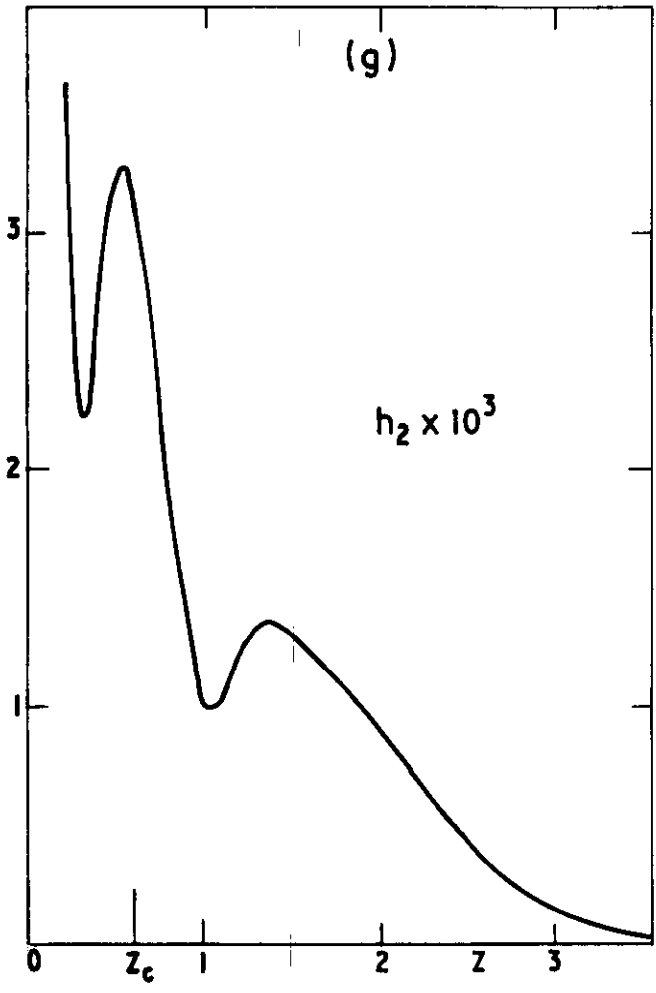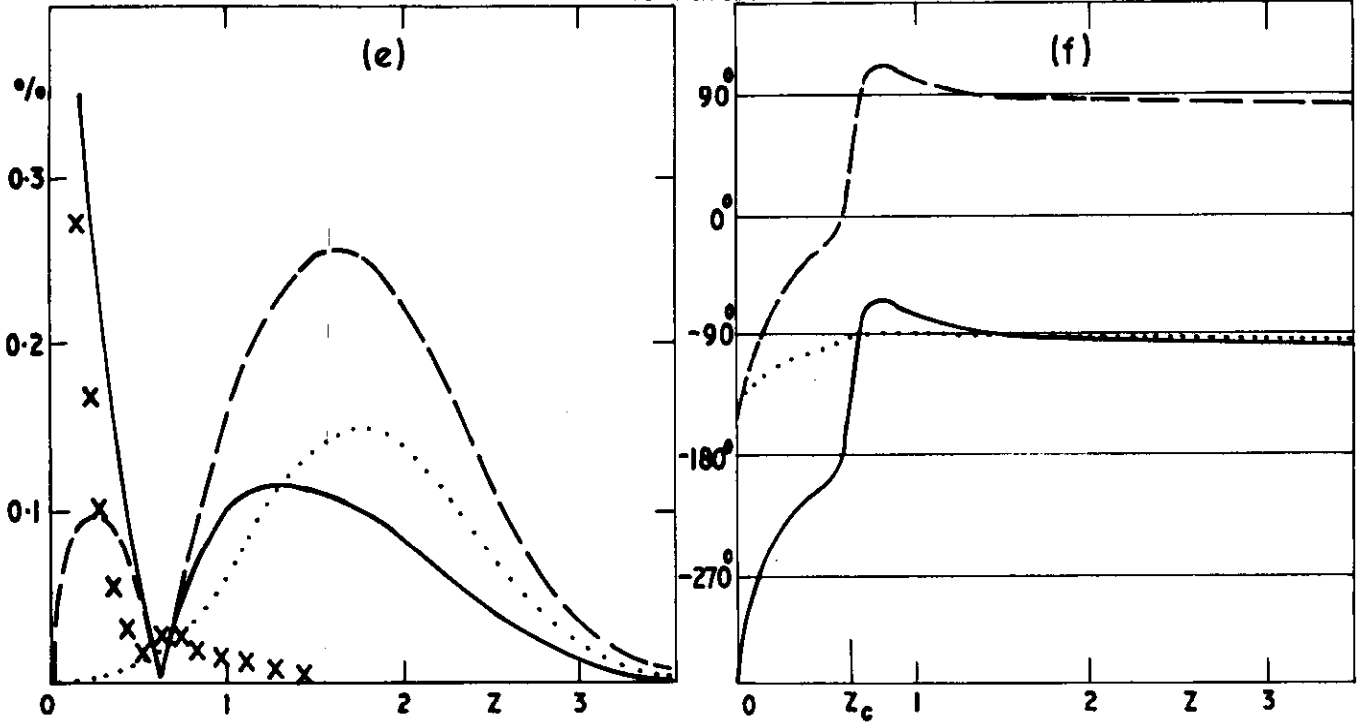
FIG. 2 (cont.)
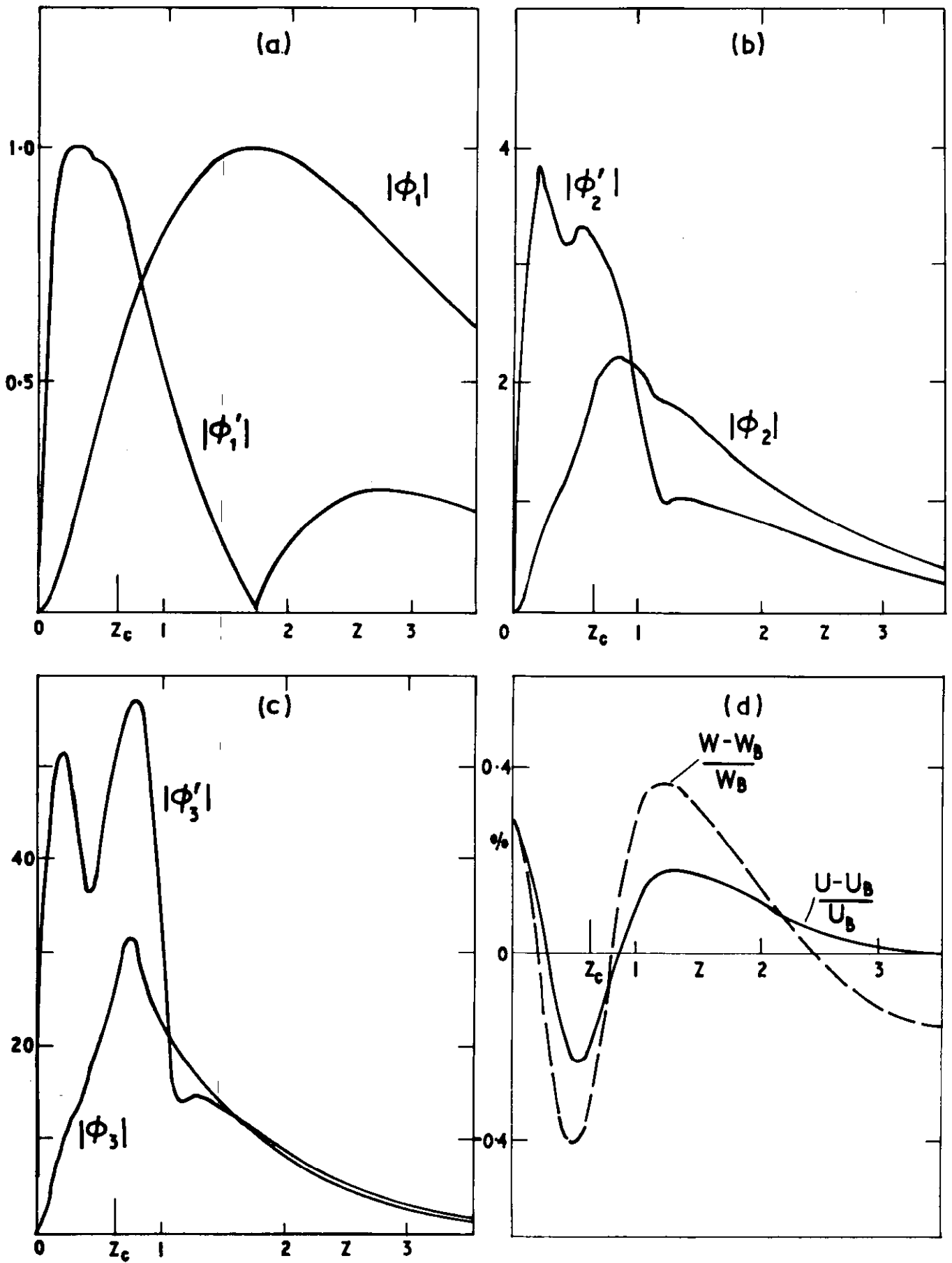
FIG.3.
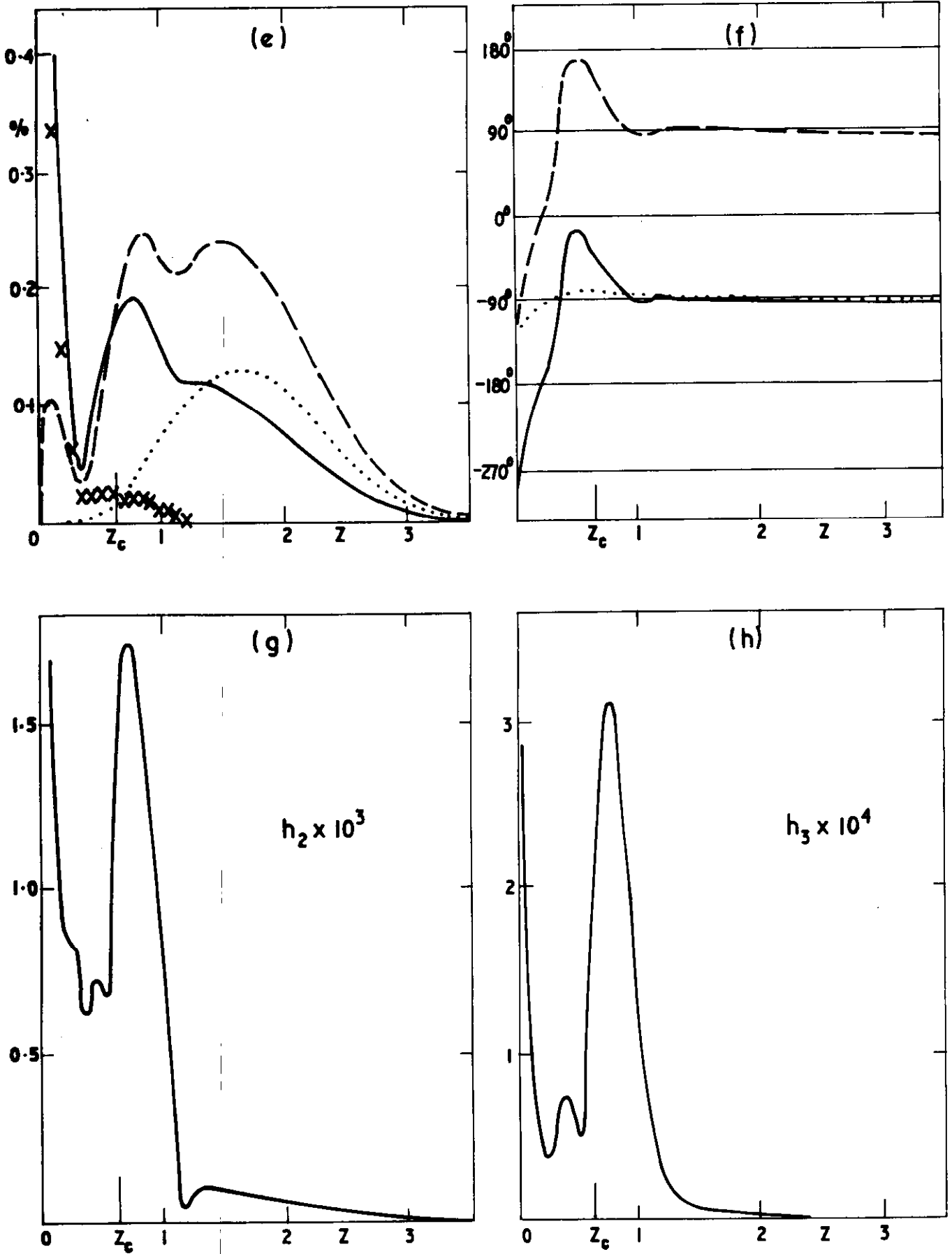
FIG. 3. (cont.)

ARC CP No.1296
February, 1973
D. Corner, M. D. J. Barry, and M. A. S. Ross
                                        - Edinburgh University
Communicated by Prof. D. Küchemann

NON-LINEAR STABILITY THEORY OF THE FLAT PLATE
BOUNDARY LAYER

A simultaneous solution of the non-linear stability
equations for the flat plate boundary layer with space
amplification has been obtained for a single
non-dimensional frequency parameter, at a series of
Reynolds numbers, and using a limited number of amplitudes
of the fundamental perturbation. The distortion of the
fundamental by the generation of second harmonic is
normally included in the solution, but some results are
                                                obtained/

obtained excluding this effect. The terms representing
the growth of boundary layer thickness are included.
The results are compared with published work on
non-linear effects in plane Poiseuille flow.

DETACHABLE ABSTRACT CARDS